Available online at www.sciencedirect.com
ScienceDirect
Journal of Hazardous Materials 149 (2007) 1–7
Journal of Hazardous Materials
www.elsevier.com/locate/jhazmat

Photocatalytic degradation of phenol in aqueous solutions by Pr-doped TiO_2 nanoparticles

Chwei-Huann Chiou, Ruey-Shin Juang *

Department of Chemical Engineering and Materials Science, Yuan Ze University, Chung-Li 32003, Taiwan

Received 29 October 2006; received in revised form 12 March 2007; accepted 12 March 2007
Available online 16 March 2007

Abstract

Photocatalytic degradation of phenol in water was examined using Pr-doped TiO_2 nanoparticles. These photocatalysts were synthesized by an acid-peptized sol–gel method from titanium tetra-isopropoxide with different concentrations of Pr(III) dopant and calcination temperatures. Several tools such as XRD, BET surface area, SEM, and EDX, were used to evaluate particle structure, size distribution, and composition. The optical absorption properties of the prepared particles were also measured. Photocatalytic activity of the particles was studied in a batch reactor containing phenol solution with 400 W UV irradiation. Parameters affecting photocatalytic process such as the catalyst crystallinity, light absorption efficiency, the dosage of catalyst, dopant and phenol concentrations were investigated. The Pr-doped TiO_2 showed high activity for photocatalytic degradation of phenol. The presence of Pr ions in the TiO_2 particles would cause a significant absorption shift towards the visible region. The degradation process was optimized using 1 g/L Pr-doped TiO_2 with a Pr(III) concentration of 0.072 mol% after 2 h irradiation. It was shown that photodegradation followed a pseudo-first-order kinetics and the rate constant changed with phenol concentration.

Keywords: Photocatalytic degradation; Phenol; Pr-doped TiO_2; Sol–gel method; Nanoparticles

1. Introduction

The presence of phenolic compounds in aqueous solutions has caused several environmental problems. A representative of this class of compounds is phenol. Sources of phenol include the discharges of chemical process industries such as coal gasification, polymeric resin production, oil refining, coking plants, paper mill, herbicides and fungicides production [1]. Phenol and their degradation products in the environment are major aquatic pollutants. When phenol-containing water is chlorinated, toxic polychlorinated phenols can be formed; hence, such effluent requires proper treatment before being discharged into the environment. Since they are stable and soluble in water, their removal to reach safety levels in the range 0.1–1.0 mg/L is not easy [2]. Traditional methods such as solvent extraction, activated carbon adsorption, and common chemical oxidation often suffer from serious drawbacks including high cost or formation of hazardous by-products [1,3]. Biological degradation is environmental friendly and cost effective; but it is usually time-consuming [3]. Among the methods available, oxidative degradation using photocatalysts appears cost effective, which has thus been an increasingly important process in pollution prevention [4–7].

Photocatalytic degradation of such organic pollutants with TiO_2 semiconductor has been proved to be the most efficient and popular method because it is a stable and low-cost photosensitized material [8]. The effective photoexcitation of TiO_2 particles requires the application of light with energy higher than its band gap energy; moreover, such photoexcitation results in the formation of electrons (e^-) in the conduction band and positive holes (h^+) in the valence band, and formation of OH radicals [9]. Photogenerated electron-hole pairs also recombine; therefore, inhibiting the recombination of electron–hole pairs and prolonging lifetime of carriers are essential for improving the efficiency of net charge transfer at the semiconductor/electrolyte interface. The hydroxyl ions (OH^-) are the likely traps for holes, leading to the formation of hydroxyl radicals that are strong oxidizing agents, while the traps for electrons are adsorbed oxygen species, leading to the formation of superoxide species (O_2^-) which are unstable [6]. The reactive radical species generated

* Corresponding author. Tel.: +886 3 4638800x2555; fax: +886 3 4559373.
E-mail address: rsjuang@ce.yzu.edu.tw (R.-S. Juang).

0304-3894/$ – see front matter © 2007 Elsevier B.V. All rights reserved.
doi:10.1016/j.jhazmat.2007.03.035

(OH^-, O_2^-) attack phenolic molecules present in suspensions and cause its hydroxylation, oxidation, and finally mineralization occur in forming to carbon dioxide and water [10,11].

Several researchers have studied the photocatalytic degradation of phenol and chlorinated phenols in aerated suspensions of TiO_2 upon illumination with near-UV light [12–14]. In most of the above studies, the Langmuir–Hinshelwood model was often applied to characterize the reaction [15,16], which describes the degradation rate in terms of the disappearance of compounds or the formation of CO_2. It has been indicated that catalyst dosage, initial concentration of organic pollutants, pH, UV light intensity, and concentration of charge trapping species are the main parameters affecting the degradation rate of phenol in TiO_2 suspension [17–19]. Previous work generally uses near-UV as the light source; however, only about 3% of the solar light is absorbed in solar energy applications [20]. Tryba et al. [21] have used an activated carbon as adsorbent, combined with TiO_2 photocatalyst, to improve the efficiency of phenol degradation.

In recent years, many groups have examined the effect of metal doping on photocatalytic properties of TiO_2. The incorporation of transition metals into TiO_2 crystal lattice alters the photoreactivity by shifting the band gap of the catalysts into the visible region [22–25]. For instance, Blazkova et al. [26] doped Pt in TiO_2 immobilized on glass fibers by sol–gel technique to improve phenol photodegradation under UV irradiation. The reflectance spectra of TiO_2-containing Fe have shown increased absorption dependence on annealing temperature and Fe concentration [27]. In addition to the methods of catalyst preparation, the photoactivity of the doped TiO_2 catalysts depends substantially on the nature of the dopant and its concentration [28,29]. Iwasaki et al. [30] reported that TiO_2 doped with a small amount of Co^{2+} has high photocatalytic activity under UV–vis light irradiation at a Co^{2+} doping concentration of 0.03 mol%. In the same subject, Barakat et al. [6] also reported a Co^{3+} doping concentration of 0.036 mol% in TiO_2 particles.

There are many reports on transition metal and noble metal dopants in TiO_2 particles previously. To our knowledge, the doping of rare earth metals, particularly Pr(III), in TiO_2 and their catalytic properties have seldom been presented so far [31]. In this work, we synthesized the Pr-doped TiO_2 nanoparticles *via* a sol–gel technique with various Pr^{3+} concentrations and annealing temperatures. The photocatalytic activity of the prepared Pr-doped TiO_2 was evaluated via the degradation of phenol in aqueous solutions under 400 W UV irradiation. Parameters affecting photodegradation process such as catalyst crystallinity, optical absorption, concentration of the catalyst and dopant, and phenol concentration were examined.

2. Materials and methods

2.1. Materials and solutions

TiO_2 nanoparticles were prepared using 0.12 mol titanium tetra-isopropoxide (Ti[*iso*-OC_3H_7]$_4$, Acros 98%) in a mixture of 2 mol% ethanol (Merck 99.8%) and water. The suspension was stirred for 6 h at room temperature, followed by several centrifuge and washing steps with deionized water (Milli-Q, Millipore). The colloidal solution was then diluted with deionized water and the pH was adjusted to 1.8 by adding 0.1 M HNO_3 (Merck 65%). Pr-doped TiO_2 particles containing 0.018–0.22 mol% Pr^{3+} dopant were synthesized *via* the acid-peptized sol–gel formation method at 85 °C and were calcined at different temperatures [32]. The dopant stoichiometry was controlled by dissolving the precursor $Pr(NO_3)_3{\cdot}5H_2O$ (Acros 99.9%) in deionized water prior to the drop-wise addition of TiO_2 colloidal solution. The resulting suspension was stirred for 18 h at 85 °C, and was allowed to rest and cool to room temperature for settling the precipitate. The precipitate was separated and collected by centrifuge and washing steps with deionized water to remove contaminants. The powder samples were dried from room temperature to 100 °C in an oven and then annealed for 6 h in a tube furnace operating between 100 and 800 °C in ambient atmosphere. During this process, the samples were transformed from anatase to rutile phase. The calcined particles were finally pulverized with mortar and pestle, followed by passing through a 270 mesh.

The reagent-grade phenol was purchased from Merck Co. (99.5% purity). All other chemicals used in this work were also of reagent-grade quality. The light source used was a water-cooled 400 W high-pressure mercury lamp (HL400EH-5, SEN, Japan). The spectral irradiance of the UV lamp ranges from 253.7 to 577 nm, with three dominant peaks locating at 365, 546, and 577 nm, and the illumination distance is 80 mm. The light intensity of the UV lamp used for photodegradation experiments was recorded with a UV–vis spectrophotometer (Shimadzu, UV-2501PC).

2.2. Characterization

The Brunauer–Emett–Teller (BET) surface area of the Pr-doped TiO_2 catalysts was measured from N_2 sorption isotherm at 77 K using a Micrometrics ASAP2010 sorption analyzer. The Barrett–Joyner–Halenda (BJH) approach was applied to obtain pore size distribution from the desorption data. The samples were degassed at 150 °C for 5 h to remove any physically sorbed gases or vapors prior to the measurements. The crystalline phases present in the sample were identified by X-ray diffraction (XRD) analysis. A Siemes D8 XRD system generating monochromatic Cu Kα radiation with continuous scanning mode at a rate of 2 min^{-1} and the operating conditions of 40 kV and 40 mV was used to obtain XRD patterns. Scanning electron microscopy (SEM, Hitachi S-4800) was applied to observe the morphology of the catalysts. The dopant concentration was verified by energy dispersive X-ray analysis (EDX, Horiba 7593H). Finally, a diffusive reflective UV–vis spectrophotometer (Shimadzu UV-2501PC) was employed to measure the absorbance and estimate the band gap of the catalysts. The samples were diluted with methanol, and the resulting solution was sonicated before the measurements.

2.3. Photodegradation experiments

Degradation experiments were conducted in a batch photocatalytic reactor. This small-scale system consisted of a cylindrical

Pyrex-glass cell with 1.0 L capacity (100 mm inside diameter, 200 mm height). A 400 W high-pressure mercury lamp was placed in a 50 mm diameter quartz tube. Both the lamp and tube were then immersed in the photoreactor cell with a light path of 80 mm. The photocatalytic reactor was filled with 0.8 L of 12.5–200 mg/L phenol solution, to which 0.2–1.0 g/L of the Pr-doped TiO_2 particles were added. The pH value of the solution was measured to be 6.5–6.8 using a digital pH meter (Horiba, F-23) without any adjustment. The whole reactor was cooled with a water-cooled jacket on its outside, and the temperature was kept constant at 25 °C.

The compressed air was purged into the solution by bubbling it from the bottom to maintain an aerobic condition. The magnetic stirrer was employed to keep the suspensions uniform. Solutions were radiated by UV–vis light for specific time intervals. Experiments were performed for 120 min, and the liquid samples (5 mL) were taken at preset time intervals (every 30 min). The sample was subjected to filtration through a 0.2 μm syringe filter (Millipore, cellulose acetate membrane) to remove particles before HPLC analysis of phenol concentration. The column used was a Merck LichroCART 250-4 (250 mm length, 4 mm diameter), packed with LiChrospher 100 RP-18e. A mixture of acetonitrile (70%, v/v) and deionized water was used as the mobile phase at a flow rate of 1.0 mL/min. An aliquot of 50 μL sample was injected using Rheodyne valve and analyzed at a wavelength of 270 nm with an UV detector (Perkin Elmer, Series 200). Each experiment was duplicated. The reproducibility of the concentration measurements is mostly within 4%.

3. Results and discussion

3.1. Characteristics of the catalysts

The influence of Pr doping concentration on the transformation of anatase (A) to rutile (R) phases at different calcination temperatures was determined by XRD method. The weight fraction of rutile in the samples was calculated based on the relationship between the integrated intensities of anatase (1 0 1) and rutile (1 1 0) peaks. Fig. 1 shows typical XRD patterns obtained from the samples with 0.072 mol% Pr. The samples were calcined at 100, 200, 400, 500, 600, and 800 °C, respectively. These patterns indicate that the samples annealed at 100–400 °C become crystalline with dominantly anatase structure. Upon annealing at 500–600 °C the samples possess both anatase and rutile structures, whereas the samples annealed at 800 °C are completely transformed to the rutile structure. Also, the small peaks related to the $PrTiO_3$ phase start to appear with the formation of rutile. It is noted that the BET surface area of the sample annealed at 600 °C is 40 m^2/g.

In fact, Barakat et al. [6] prepared the Co-doped TiO_2 nanoparticles by a sol–gel technique from $TiCl_4$ with different concentrations of Co^{3+} dopant and calcination temperatures. They reported that with 0.036 mol% Co the particles annealed up to 400 °C are amorphous and become crystalline with dominantly anatase structure upon annealing at 600 °C. It is reported that anatase with a band gap of 3.2 eV is more efficient as a photocatalyst than rutile [6,33]. Thus, Fig. 1 indicates that to obtain the anatase phase of TiO_2 particles a much lower annealing temperature is sufficient using the present acid-peptized sol–gel method.

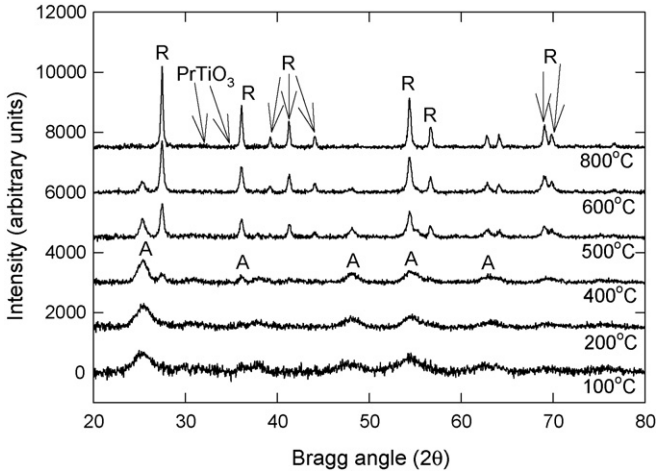

Fig. 1. XRD patterns for 0.072 mol% Pr-doped TiO_2 samples at different calcination temperatures: (a) 100 °C, 100% A; (b) 200 °C, 100% A; (c) 400 °C, 85% A, 15% R; (d) 500 °C, 69% A, 31% R; (e) 600 °C, 40% A, 60% R; (f) 800 °C, 100% R (A: anatase; R: rutile).

It is recognized that the optical properties of Pr-doped TiO_2 (obtained form diffusive reflectance spectra) directly affect the photo reactivity according to the light absorption efficiency and functioning wavelength range [6]. The photoreactivity of Pr-doped TiO_2 is greatly improved by the high efficiency and wide range of light absorption, due to the increased photogeneation rate of charge-transfer between Pr^{3+} electrons and the TiO_2 conduction or valence band [31]. Fig. 2 shows the absorption spectra for Pr-doped TiO_2 samples with different Pr concentrations. The light absorption in the region between 350 and 520 nm shifts the absorption curve to a longer wavelength compared to that of undoped TiO_2. The absorption reaches a maximum for the sample with 0.072 mol% Pr. Further increase in the Pr^{3+} con-

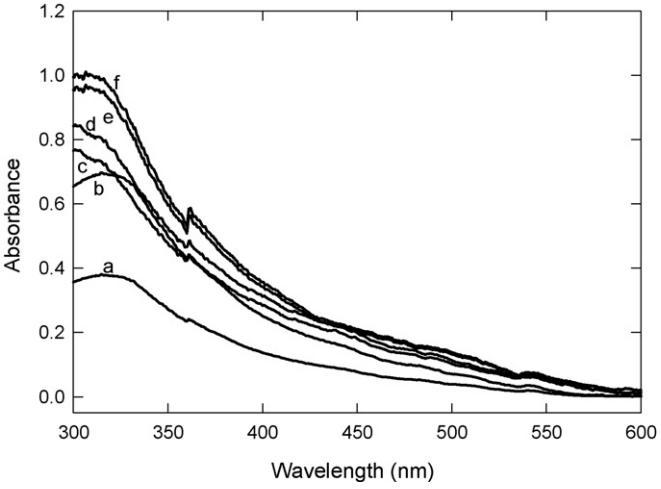

Fig. 2. Effect of Pr doping concentration on optical absorption of TiO_2: (a) 0% Pr, (b) 0.22 mol% Pr, (c) 0.143 mol% Pr, (d) 0.018 mol% Pr, (c) 0.036 mol% Pr, and (f) 0.072 mol% Pr.

centration results in the shifting of absorption curves toward the shorter wavelength (not shown). The band gap can be estimated by extrapolating the rising portion of the absorption spectrum to the abscissa at zero absorption [9]. The band gap of laboratory-made TiO_2 was 3.21 eV, which is different from that of the Pr/TiO_2 between 2.80 and 3.10 eV. The effect of higher dopant concentration on the lifetime of the charged carrier has been discussed [23,30]. Increasing dopant concentration above an optimal value would result in forming the recombination centers or trapping the charges for a long time, thereby decreasing the photodegradation efficiency [6].

Morphology of the supports and the supported catalysts were determined by SEM micrographs. It is observed from Fig. 3 that an increase in annealing temperature leads to a larger TiO_2 particle; however, all Pr-doped TiO_2 samples reveal similar shapes with a particle size distribution of 10–50 nm. The molar ratio of Pr to Ti is estimated from the EDX semi-quantitative acquisition, ranging from 0.009 to 0.044 for 0.018–0.22 mol% Pr. Spot EDX analysis reveals that most Pr is present on the surface of the TiO_2 support.

3.2. Photocatalyic degradation

The efficiency of phenol photodegradation as a function of operating parameters is shown in Figs. 4–8. To study the effect of catalyst structure on photodegradation, samples annealed at different temperatures that show different crystal structures were used. Fig. 4 illustrates the results. The highest degradation is achieved with the samples annealed at 600 °C, which is primarily because the crystalline includes both anatase and rutile structures. The band gap energy of anatase sample measured by UV–vis spectrophotometry was found to be 3.2 eV, which is the same as that of the bulk TiO_2. The samples annealed at 800 °C are rutile structure. They give lower degradation efficiency than those annealed at 400 and 600 °C, which are anatase and anatase-rutile mixture, respectively. As have been indicated earlier, the

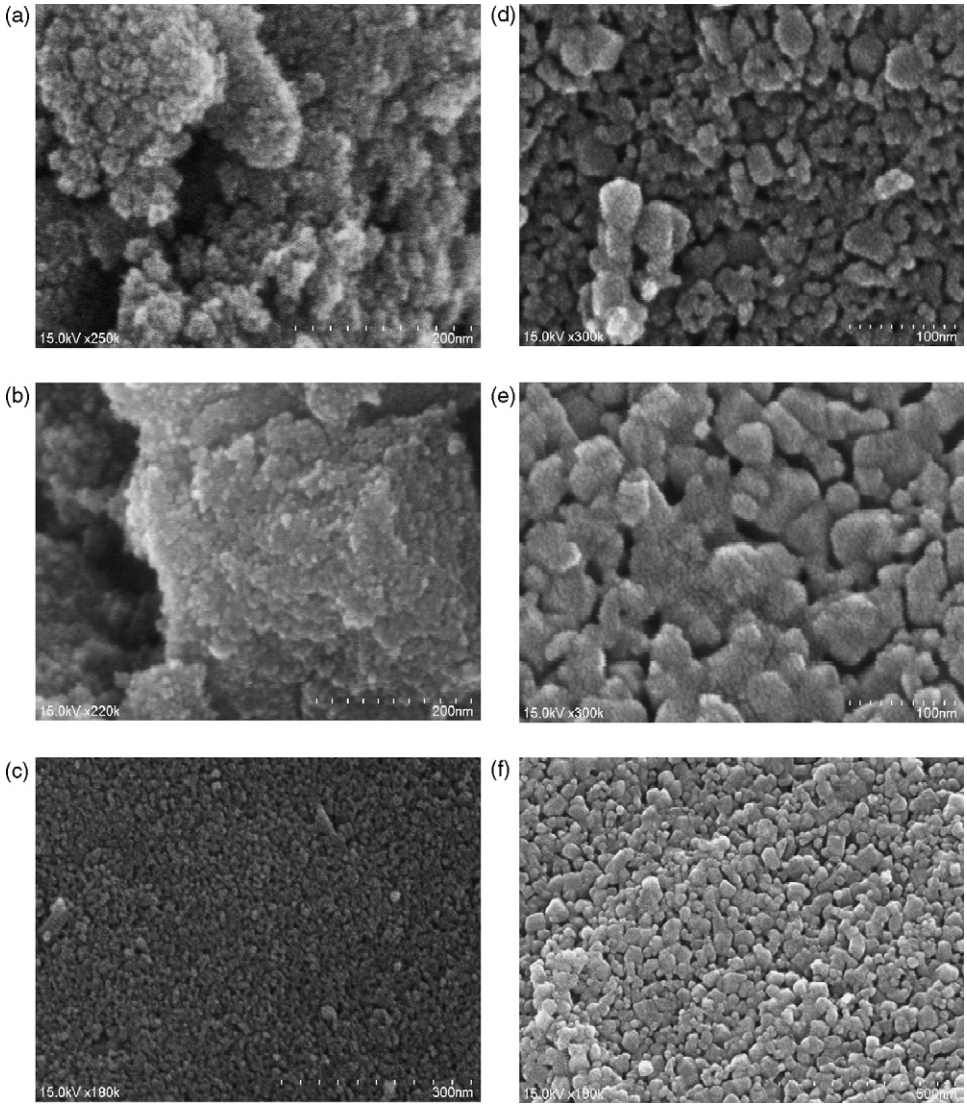

Fig. 3. SEM micrographs of 0.072 mol% Pr-doped TiO_2 samples annealed at (a) 100 °C, (b) 200 °C, (c) 400 °C, (d) 500 °C, (e) 600 °C, and (f) 800 °C.

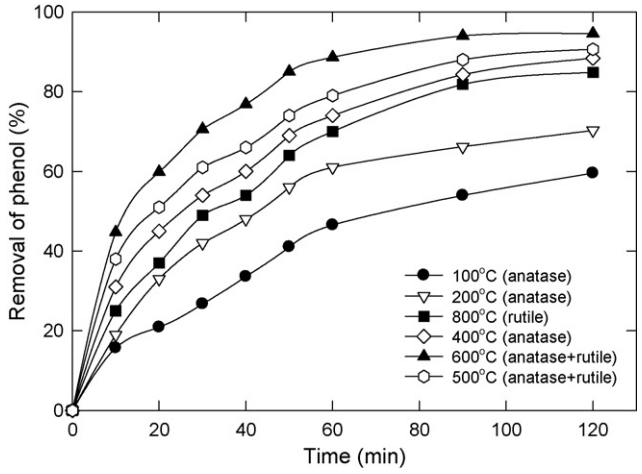

Fig. 4. Effect of the calcination temperature of Pr-doped TiO_2 on phenol photodegradation (0.072 mol% Pr, catalyst dosage 1.0 g/L, 50 mg/L phenol).

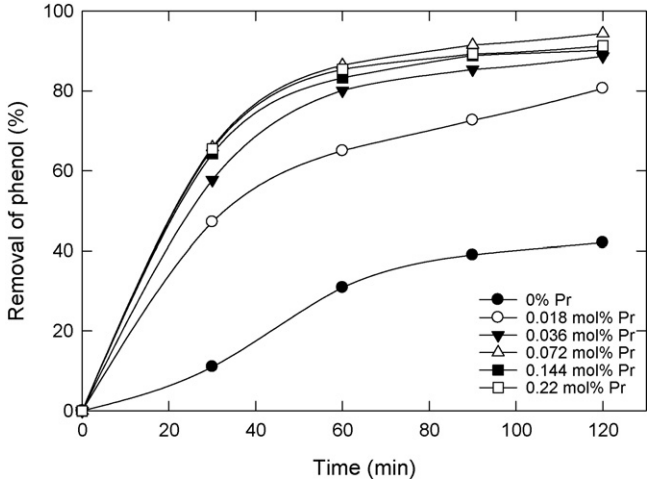

Fig. 5. Effect of the Pr doping concentration on phenol photodegradation (catalyst dosage 1.0 g/L, 50 mg/L phenol).

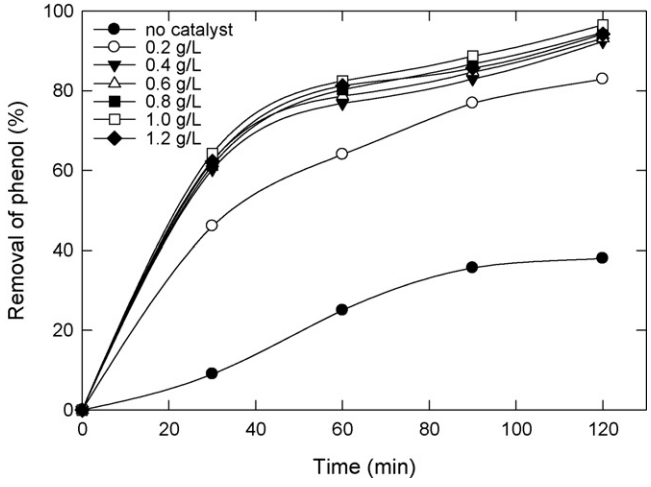

Fig. 6. Effect of the dosage of Pr-doped TiO_2 on phenol photodegradation (0.072 mol% Pr, 50 mg/L phenol).

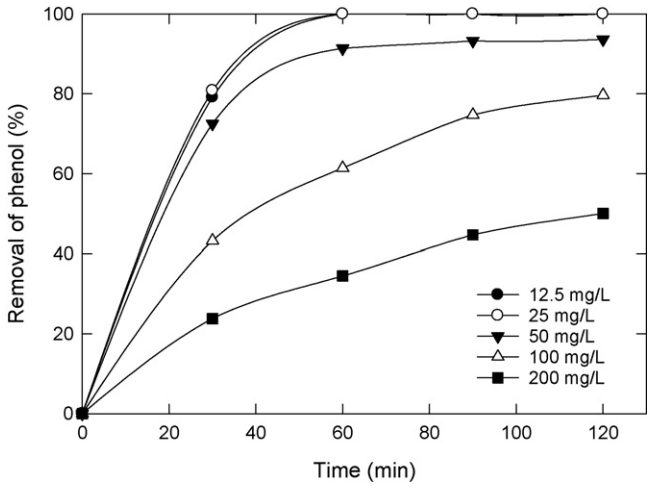

Fig. 7. Effect of phenol concentration on its photodegradation rate (0.072 mol% Pr, catalyst dosage 1 g/L).

TiO_2 particles with anatase structure have a better photocatalytic activity [6,33,34].

Tsai and Cheng [35] have reported that, between the laboratory-made anatase and rutile TiO_2, anatase reveals better photocatalytic activity in decomposition of phenolic pollutants. However, the present results show that the Pr-doped TiO_2 particles containing both anatase and rutile structures have the highest activity. This observation matches the work of Ohno et al. [36] that the co-existence of anatase and rutile structures leads to a synergistic effect. Also, the catalytic activity of the catalyst strongly depends on its calcination temperature. Iwasaki et al. [30] also confirmed that the catalytic activity of Co^{3+}-doped TiO_2 declines when annealing temperature rises over 600 °C where the rutile structure and a new compound $CoTiO_3$ are formed. In fact, a similar compound $PrTiO_3$ is found in our XRD patterns (Fig. 1).

Fig. 5 shows the effect of Pr^{3+} dopant concentration (0.018–0.22 mol%) on phenol photodegradation. For a solution containing initially 50 mg/L phenol after 2 h UV irradiation,

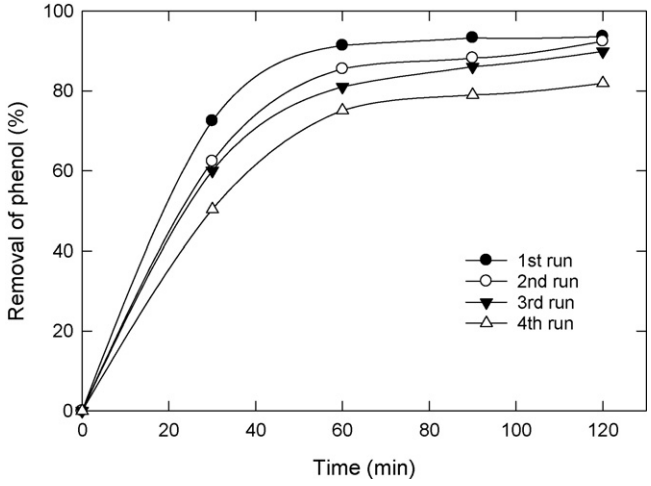

Fig. 8. Reproducibility of the Pr-doped TiO_2 catalyst for phenol photodegradation at comparable rates for four cycles (0.072 mol% Pr, catalyst dosage 1 g/L, 50 mg/L phenol).

42% of phenol is degraded with the undoped sample. The degradation efficiency increases with increasing Pr concentration, and a maximum of 94.4% is obtained with sample containing 0.072 mol% Pr that was annealed at 600 °C. A further increase in Pr concentration to 0.22 mol% leads to a slight decrease in degradation efficiency to 91.3%. The variation of degradation efficiency with Pr concentration could be understood by the following mechanism. Under the irradiation of Pr-doped TiO_2 particles, Pr^{3+} works as electron scavenger, which may react with the superoxide species and prevent the holes–electrons (h^+/e^-) recombination, and thus increases photo-oxidation efficiency [6]. The possible reaction is represented below:

$$Pr^{3+} + O_2{}^- (ads) \rightarrow Pr^{2+} + O_2 (ads) \quad (1)$$

On the other hand, a higher Pr concentration results in a decrease in transformation temperature of anatase to rutile phases and the formation of $PrTiO_3$ compound. This might lead to a further decrease in degradation efficiency. Iwasaki et al. [30] and Choi et al. [37] have actually confirmed the retarding effect of increasing Co^{3+} doping concentration on the photocatalytic activity of TiO_2 under UV irradiation.

Burns et al. [38] have studied photodegradation of 2-chlorophenol using sol–gel synthesized Nd-doped TiO_2 under UV irradiation. They reported that doping TiO_2 with Nd^{3+} reduces the degradation time because of the difference in the ionic radii of Nd^{3+} and Ti^{4+}. Much larger substitutional Nd will cause localized charge perturbation and formation of oxygen vacancies which act as electron traps. This is also the case here. The time required to remove a certain percent of phenol is much shorter using the present Pr-doped TiO_2 particles, in contrast to the use of other transition metal-doped TiO_2 particles [5,8,13,21,26]. For example, with 0.072 mol% Pr-doped TiO_2 it takes merely 45 min to degrade 80% of initially 50 mg/L phenol (Fig. 5); however, the degradation was smaller than 80% with undoped and other metal-doped TiO_2 particles under comparable conditions (reaction time, phenol concentration, etc.). On the other hand, the present Pr-doped TiO_2 yields satisfactory removal of phenol (say, >90%) in a neutral solution, whereas the corresponding efficiency was achieved in more acidic or basic solutions using other metal-doped TiO_2 particles [6,26,34].

The effect of the dosage of Pr-doped TiO_2 on phenol degradation is illustrated in Fig. 6. In the absence of the catalyst, about 38% of initially 50 mg/L phenol is removed at pH 6.58 after 2 h of UV irradiation (The phenol degradation efficiency of the same catalyst without bubbling is 27%). This is purely a photolysis process. The rate of phenol photolysis is almost the same as that of photodegradation using the undoped TiO_2 samples (lowest curve of Fig. 5). It is expected that phenol degradation increases with increasing the dosage of 0.072 mol% Pr-doped TiO_2, and reaches a maximum of 96.5% at a dosage of 1.0 g/L. However, a further increase in catalyst dosage (e.g., 1.2 g/L) slightly reduces the photodegradation efficiency. In principle, the photodegradation rate of pollutants is affected by not only the active sites but also the photo-absorption of the catalyst used. Adequate dosage of the photocatalyst increases the generation rate of electron/hole pairs for enhancing photodegradation, but a high dosage of the photocatalysts will decrease the light penetration by the suspension [39] and reduce the degradation rate.

Fig. 7 shows the influence of initial phenol concentration on its photodegradation. As expected, the degradation efficiency is higher when phenol concentration is lower. Phenol degradation may be controlled by the limited numbers of surface sites of the photocatalyst. At concentrations below 25 mg/L, phenol can be totally decomposed within 1 h. The present results indicate that photocatalytic oxidation process is rather promising at low pollutant concentrations. This is also the case for heterogeneous catalytic systems where the reaction occurs at the interface between the two phases. The reaction can be represented mechanistically and stoichiometrically as follows [7]:

$$\underset{(C_6H_5OH)}{\text{phenol}} \xrightarrow{h\nu} \underset{C_6H_4(OH)_2}{\text{catechol}} \xrightarrow{h\nu} \text{intermediates} \xrightarrow{h\nu} CO_2,\ H_2O \quad (2)$$

$$C_6H_5OH + 7O_2 \rightarrow 6CO_2 + 3H_2O \quad (3)$$

The reproducibility of the catalyst for phenol photodegradation in a four-cycle experiment is shown in Fig. 8. After each degradation experiment, the concentration of phenol was adjusted back to its initial value of 50 mg/L. A small but gradual decrease in activity of the catalyst is found after the first two cycles, after that the activity maintains essentially unchanged. The degradation efficiencies are 93.6, 92.4, 89.9, and 81.9% in the first to fourth runs, respectively. The repeatability of phenol degradation indicates that this is indeed a photocatalytic reaction. For the same mass of catalyst, an increase in phenol concentration increases the reaction intermediates adsorbed onto the catalyst. The active sites will be occupied to form a monolayer; as the result, the rate is decreased.

A Langmuir–Hinshelwood type of kinetic model is used here to describe the concentration effect on its degradation rate [15,16]. The apparent first-order rate constants are obtained to be 0.051, 0.049, 0.038, 0.014, and 0.006 min^{-1} at pH 6.58 and initial phenol concentration of 12.5, 25, 50, 100, and 200 mg/L, respectively (not shown). The variation of apparent rate constant with phenol concentration is consistent with previous result [13]. Xu et al. [31] have actually indicated that photodegradation of nitrite over Gd^{3+}-doped TiO_2 and Degussa P-25 (undoped TiO_2) samples follows pseudo-first-order kinetics. However, the photodegradation over Sm^{3+}-, Ce^{3+}-, Er^{3+}-, Pr^{3+}-, La^{3+}-, and Nd^{3+}-doped TiO_2 samples obey the zero-order kinetics. Further studies should be undertaken to check such inconsistent kinetic behavior with Pr-doped TiO_2 although the nature of the reactants could be play an important role.

4. Conclusions

The Pr-doped TiO_2 nanoparticles with a composition of $Ti_{1-x}Pr_xO_2$ ($x = 0.018$–0.22) were prepared *via* an acid-peptized sol–gel method. The anatase phase of Pr-doped TiO_2 particles could be formed even annealed at 100 °C. Particles that were annealed at 600 °C revealed the highest phenol photodegradation efficiency, primarily because they included both anatase and rutile structures. Light absorption reached a maximum for

the particles with 0.072 mol% Pr, which was consistent with the trends of phenol photodegradation efficiency. Light absorption measurements also confirmed that the presence of 0.072 mol% Pr doping in TiO_2 caused significant absorption shift into the visible region compared to the use of undoped TiO_2 particle. Using 0.072 mol% Pr-doped TiO_2, phenol degradation with an UV irradiation of 400 W followed the pseudo-first-order kinetics. The difference of apparent rate constant between initial phenol concentration of 12.5 and 200 mg/L was nearly nine-fold. At a dosage of 1.0 g/L, 0.072 mol% Pr-doped TiO_2, about 99 and 50% of phenol was degraded after 2 h irradiation at an initial concentration of 12.5 and 200 mg/L, respectively. The present results demonstrated the promising photocatalysis potential of the Pr-doped TiO_2 particles, at least for phenol, due to their relatively faster degradation.

References

[1] J.W. Pattersom, Wastewater Treatment Technology, Ann Arbor Science Pub. Inc., Ann Arbor, MI, 1985, pp. 199–215.

[2] V.M. Brown, D.H.M. Jordan, B.A. Tiller, The effect of temperature on the acute toxicity of phenol to rainbow trout in hard water, Water Res. 1 (1967) 587–597.

[3] R.L. Autenrieth, J.S. Bonner, A. Akgerman, E.M. McCreary, Biodegradation of phenolic wastes, J. Hazard. Mater. 28 (1991) 29–53.

[4] C. Hu, Y.Z. Wang, H.X. Tang, Destruction of phenol aqueous solution by photocatalysis or direct photolysis, Chemosphere 41 (2000) 1205–1209.

[5] G. Colon, J.M. Sanchez-Espana, M.C. Hidalgo, J.A. Navio, Effect of TiO_2 acidic pretreatment on the photocatalytic properties for phenol degradation, J. Photochem. Photobiol. A: Chem. 179 (2006) 20–27.

[6] M.A. Barakat, H. Schaeffer, G. Hayes, S. Ismat-Shah, Photocatalytic degradation of 2-chlorophenol by Co-doped TiO_2 nanoparticles, Appl. Catal. B: Environ. 57 (2005) 23–30.

[7] M.M. Halmann (Ed.), Photodegradation of Water Pollutants, CRC Press, New York, 1996, pp. 83–86.

[8] D. Fabbri, A.B. Prevot, E. Pramauro, Effect of surfactant microstructures on photocatalytic degradation of phenol and chlorophenols, Appl. Catal. B: Environ. 62 (2006) 21–27.

[9] I.H. Tseng, W.C. Chang, J.C.S. Wu, Photoreduction of CO_2 using sol–gel derived titania and titania-supported copper catalysts, Appl. Catal. B: Environ. 37 (2002) 37–48.

[10] V.B. Alzbeta, E. Borova, M. Ceppan, R. Fiala, The influence of dissolved metal ions on photocatalytic degradation of phenol in aqueous TiO_2 suspensions, J. Mol. Catal. A: Chem. 98 (1995) 109–116.

[11] M.I. Litter, Heterogeneous photocatalysis transition metal ions in photocatalytic systems, Appl. Catal. B: Environ. 57 (1999) 89–114.

[12] T.R.N. Kutty, S. Ahuja, Retarding effect of surface hydroxylation on titanium(IV) oxide photocatalyst in the degradation of phenol, Mater. Res. Bull. 30 (1995) 233–241.

[13] S. Lathasree, A.N. Rao, B. Sivasankar, V. Sadasivam, K. Rengaraj, Heterogeneous photocatalytic mineralization of phenols in aqueous solutions, J. Mol. Catal. A: Chem. 223 (2004) 101–105.

[14] D.W. Chen, A.K. Ray, Photocatalytic kinetics of phenol and its derivatives over UV irradiated, Appl. Catal. B: Environ. 23 (1999) 143–157.

[15] A.V. Petukhov, Effect of molecular mobility on kinetics of an electrochemical Langmuir–Hinshelwood reaction, Chem. Phys. Lett. 277 (1997) 539–544.

[16] R.A. Doong, C.H. Chen, R.A. Maithreepala, S.M. Chang, The influence of pH and cadmium sulfide on photocatalytic degradation of 2-chlorphenol in titanium dioxide suspension, Water Res. 35 (2001) 2873–2880.

[17] G.L. Puma, P.L. Yue, Effect of radiation wavelength on the rate of photocatalytic oxidation of organic pollutants, Ind. Eng. Chem. Res. 41 (2002) 5594–5600.

[18] I. Ilisz, Z. Laszlo, A. Dombi, Investigation of the photodecomposition of phenol in near-UV-irradiated aqueous TiO_2 suspension. I. Effect of charge-trapping species on the degradation kinetics, Appl. Catal. A: Gen. 180 (1999) 25–33.

[19] K. Mogyorosi, A. Farkas, I. Dekany, TiO_2-based photocatalytic degradation of 2-chlorophenol adsorbed on hydrophobic clay, Environ. Sci. Technol. 36 (2002) 3618–3624.

[20] B. Bayarri, J. Gimenez, D. Curco, S. Esplugas, Photocatalytic degradation of 2,4-dichlorophenol by TiO_2/UV: kinetics, actinometries and models, Catal. Today 101 (2005) 227–236.

[21] B. Tryba, A.W. Morawski, M. Inagaki, Application of TiO_2-mounted activated carbon on the removal of phenol from water, Appl. Catal. B: Environ. 41 (2003) 427–433.

[22] F.B. Li, X.Z. Li, M.F. Hou, Photocatalytic degradation of 2-mercaptobenzothiazole in aqueous La^{3+}–TiO_2 suspension for odor control, Appl. Catal. B: Environ. 48 (2004) 185–194.

[23] D. Dvoranova, V. Brezova, M.A. Malati, Investigations of metal-doped titanium dioxide photocatalysts, Appl. Catal. B: Environ. 37 (2002) 91–105.

[24] Y.Q. Wang, H.M. Cheng, L. Zhang, Y.Z. Hao, J.M. Ma, B. Xu, W.H. Li, Preparation, characterization, photoelectrochemical and photocatalytic properties of lanthanide metal-ion-doped TiO_2 nanoparticles, J. Mol. Catal. A: Chem. 151 (2000) 205–216.

[25] T. Ohno, F. Tanigawa, K. Fjihara, S. Izumi, M. Matsumura, Photocatalytic oxidation of water by visible light using ruthenium-doped titanium dioxide powder, J. Photochem. Photobiol. A: Chem. 127 (1999) 107–110.

[26] A. Blazkova, I. Csolleova, V. Brezova, Effect of light source on phenol degradation using Pt/TiO_2 photocatalysts immobilized on glass fibers, J. Photochem. Photobiol. A: Chem. 113 (1998) 251–256.

[27] J.N. Chen, Y.C. Chan, M.C. Lu, Photocatalytic oxidation of chlorophenols in the presence of manganese, Water Sci. Technol. 39 (10–11) (1999) 225–230.

[28] J.A. Navio, G. Colon, M.I. Litter, G.N. Bianco, Synthesis, characterization and photocatalytic properties of iron-doped titanium semiconductors prepared from TiO_2 and iron(III) acetylacetonate, J. Mol. Catal. A: Chem. 106 (1996) 267–276.

[29] J.A. Navio, J.J. Testa, P. Djedjeian, J.R. Padron, D. Rodriguez, M.I. Litter, Iron-doped titania powder by a sol–gel method. Part II. Photocatalytic properties, Appl. Catal. A: Gen. 178 (1999) 191–203.

[30] M. Iwasaki, M. Hara, H. Kawada, H. Tada, S. Ito, Cobalt ion-doped TiO_2 photocatalyst response to visible light, J. Colloid Interface Sci. 224 (2000) 202–204.

[31] A.W. Xu, Y. Gao, H.Q. Liu, The preparation, characterization, and their photocatalytic activities of rare-earth-doped TiO_2 nanoparticles, J. Catal. 207 (2002) 151–157.

[32] J. Krysa, M. Keppert, J. JirKovsky, V. Stengl, J. Subrt, The effect of thermal treatment on the properties of TiO_2 photocatalyst, Mater. Chem. Phys. 86 (2004) 333–339.

[33] M.A. Fox, M.T. Dulay, Heterogeneous photocatalysis, Chem. Rev. 93 (1993) 341–357.

[34] M.A. Barakat, Y.T. Chen, C.P. Huang, Removal of toxic cyanide and Cu(II) ions from water by illuminated TiO_2 catalyst, Appl. Catal. B: Environ. 53 (2004) 13–20.

[35] S.J. Tsai, S. Cheng, Effect of TiO_2 crystalline structure on photocatalytic degradation of phenolic contaminants, Catal. Today 33 (1997) 227–237.

[36] T. Ohno, K. Sarukawa, K. Tokieda, M. Matsumura, Morphology of a TiO_2 photocatalyst (Degussa P-25) consisting of anatase and rutile crystalline phases, J. Catal. 203 (2001) 82–86.

[37] W. Choi, A. Termin, M.R. Hofmann, The role of metal ion dopants in quantum-sized and charge carrier recombination dynamics, J. Phys. Chem. 98 (1994) 13669–13679.

[38] A. Burns, W. Li, C. Baker, S.I. Shah, Sol–gel synthesis and characterization of neodymium-ion doped nanostructured titania thin film, Mater. Res. Soc. Symp. Proc. 703 (2002) 193–198.

[39] R.A. Doong, W.H. Chang, Photodegradation of parathion in aqueous titanium dioxide and zero-valent iron solutions in the presence of hydrogen peroxide, J. Photochem. Photobiol. A: Chem. 116 (1998) 221–228.